Crimson Publishers
Wings to the Research

Short Communication

Diamond and Diamond-Like Carbon in Grey Cast Iron

Rainer Thomas*

Im Waldwinkel 8, D14662 Friesack, Germany

ISSN: 2576-8840

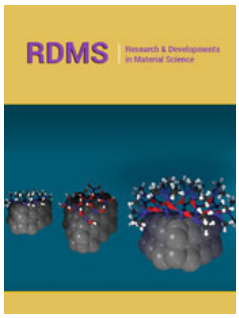

***Corresponding author:** Rainer Thomas, Im Waldwinkel 8, D-14662 Friesack, Germany

Submission: August 24, 2026
Published: September 03, 2026

Volume 23 - Issue 2

How to cite this article: Rainer Thomas*. Diamond and Diamond-Like Carbon in Grey Cast Iron. Res Dev Material Sci. 23(2). RDMS. 001057. 2026.
DOI: 10.31031/RDMS.2026.23.001057

Copyright@ Rainer Thomas, This article is distributed under the terms of the Creative Commons Attribution 4.0 International License, which permits unrestricted use and redistribution provided that the original author and source are credited.

Abstract

Acid treatment of grey cast iron sample 2 (GJS 400) yielded fragile graphite-like lamellae containing abundant spherical diamond inclusions and Diamond-Like Carbon (DLC). Microscopic observations showed that the approximately 10-30µm thick lamellae contain diamonds about 2.5µm in diameter distributed throughout their volume, including below the surface. Raman measurements identified diamond-related bands, although overlapping signals from graphite, DLC, nanodiamond, and diamond broadened the spectra, as did laser-induced carbon degradation. The lamellae's transparency and depth-dependent optical appearance indicate they are not pure graphite but include a substantial DLC component. The observations suggest a complex carbon structure formed under locally elevated pressure, possibly near the graphite-diamond equilibrium. The formation conditions and precise thermal history remain uncertain, but the findings indicate that conventional grey cast iron phase diagrams may not describe all stages of cooling.

Keywords: Grey cast iron; Diamond inclusions; Diamond-like carbon; Graphite lamellae; Raman spectroscopy; Nanodiamond; Carbon phases; High pressure; Boron phases; Phase diagrams

Introduction

During Raman spectroscopy of gray cast iron, we found small diamond crystals distributed throughout some graphite. The diamond appears to have come from preparing the cube-shaped iron sample with diamond paste. To rule out this possibility, we treated the sample with hydrochloric acid [1-3]. We rejected the first fraction because of possible contamination. In the second residue, we found, to our astonishment, graphite-like lamellae with a large number of small diamonds or Diamond-Like Carbon (DLC). In all studied grey cast iron samples, we found isolated single diamonds that were clearly distinguished from the diamond used for preparation [4]. This was also the case for a meteorite-like iron piece from the Bieleboh Mt. in Lusatia, E-Germany [2]. Besides the diamond spheres, we also found mostly colorless α-boron and various colorless to black boron carbides. Note: Boron carbide (B_4C) is typically black to dark gray at room temperature; depending on purity and form, it may appear slightly greenish-black or brownish black. At high temperature and pressure, these phases become colorless [5].

Sample Material

For this study, we used iron sample 2 (type GJS 400), a rectangular parallelepiped weighing 15.2g. Brümmer et al. [3] describe the sample material used. In the first step, we dissolved 1.90g of the sample in hydrochloric acid (25%) to remove possible diamond remnants from grinding and polishing. This fraction was rejected. In the second step, we dissolved an additional 1.60g of iron; we washed the insoluble residue with distilled water and then air-dried it. This residue served as the object of our study.

Microscopy and Raman Spectroscopy

For all microscopic and Raman spectroscopic investigations, we used a petrographic polarization microscope (BX 43) equipped with a rotating stage and coupled to an EnSpectr

Raman spectrometer R532 (Enhanced Spectrometry, Inc., Mountain View, CA, USA). For all analyses, we used a long-working-distance Olympus LMPlanFL 100× objective, which provides a measurement field of about 1µm in diameter on the sample.

We calibrated Raman-band positions before and after each measurement series using the Si band of a semiconductor-grade single-crystal silicon chip. Based on 20 repeated measurements, run-to-run reproducibility was ±0.2cm^{-1} for silicon (520.2±0.2cm^{-1}) in the range from 0 to 2000cm^{-1}. As a second reference, we used a water-clear diamond crystal from Brazil. We measured the first-order diamond line at 1333.4±0.6cm^{-1}, with a FWHM of 5.1±0.1cm^{-1} [6]. FWHM is full width at half maximum. However, scrutiny of the Brazil diamond shows small heterogeneities (different ^{13}C content). Figure 1 shows the characteristics of the Raman system used, obtained from the Brazil reference diamond.

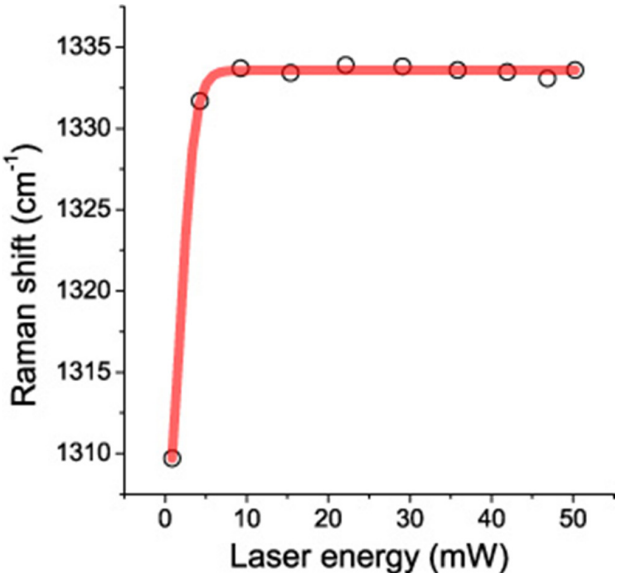

Figure 1: Raman shift (cm^{-1}) versus laser (532nm) energy (mW) obtained using the Brazil reference diamond. The sigmoid (Boltzmann) fit starts at 1302.5cm^{-1}, 0.8mW and ends at 1333.6cm^{-1} and 50mW. The correlation coefficient is R^2=0.99914.

For this study, we used conspicuous graphite lamellae with colorless spherical inclusions, as in Figure 2 in Thomas [1]. In that report, we assumed that the thickness of the lamellae was as thick as the diameter of the diamonds (≥2.5µm) because, at the place of the diamonds, the graphite lamella looks very transparent. Later studies, however, showed that this was a non sequitur. The lamellas are about 10 to 30µm thick, and the spherical diamonds are only about 2.5µm thick and can be seen deep in the sample.

Results

The graphite lamellae, about 10 to 30µm thick, contain diamond spheres about 2.5µm in diameter that permeate the entire volume of graphite. Figure 2 shows such a larger lamella. The number of diamonds is relatively large. A simple counting using the principle of Delesse [7] gives about 1*10^6 diamonds/cm^2.

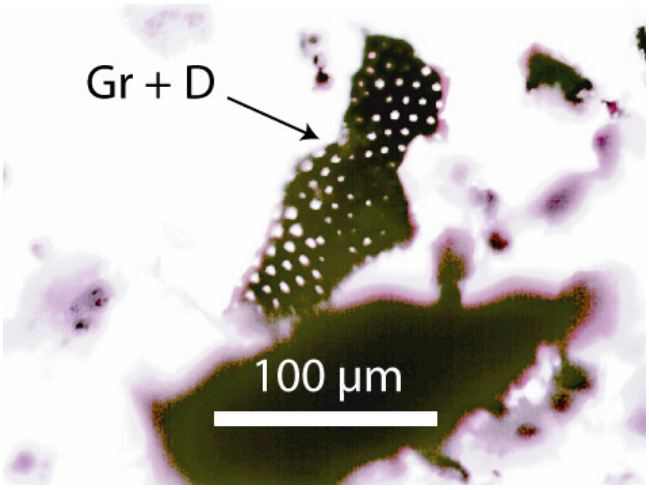

Figure 2: Large graphite (Gr) - diamond (D) lamella from the grey cast iron. If we turn the sample, we get about the same result.

Figure 3 shows a further example. Such lamellas are very fragile, and handling is not simple.

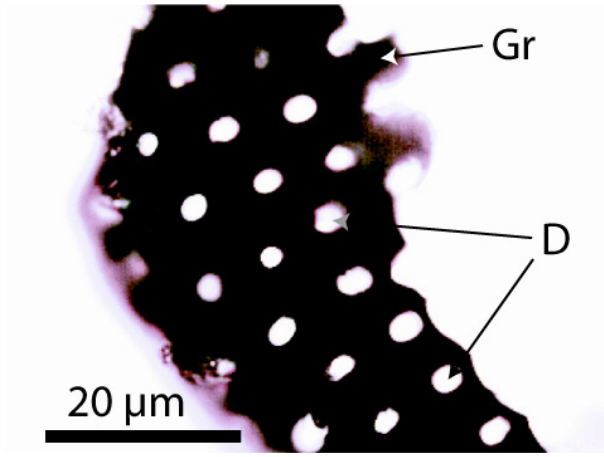

Figure 3a: Graphite (Gr) lamella with diamonds (D) from the gray cast iron sample 2.

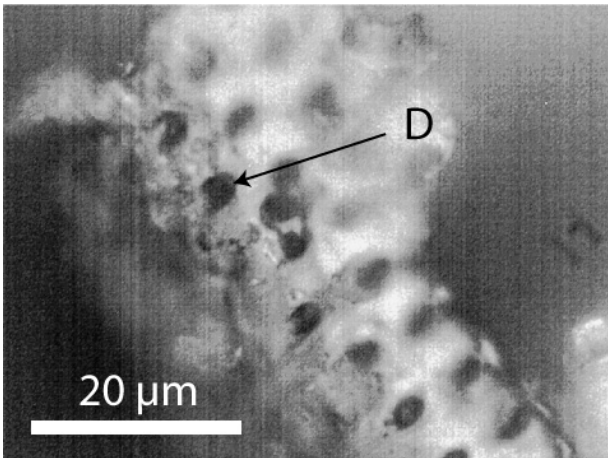

Figure 3b: Graphite lamella 2a under a reflected light microscope. The black points are diamonds (D).

Copyright © Rainer Thomas

Important is that such lamellas are relatively seldom in the residue of the solved grey cast iron. Different boron phases are more frequent.

Focusing on the depths of the graphite lamellas shows that there are also diamonds under the surface (Figure 4). Why such diamonds are also white is not completely clear. Figure 5 shows one lamella, focused on different depths. The results of the Raman measurements on diamonds in such a lamella are shown in Figure 6.

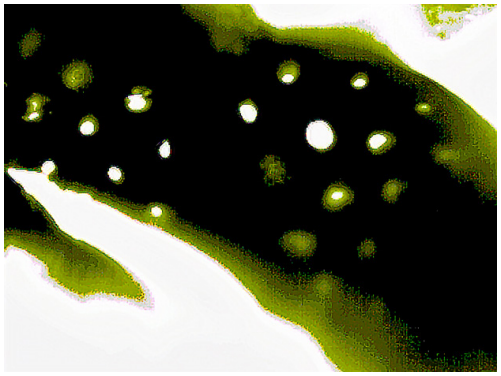

Figure 4: This figure of a lamella clearly shows that diamonds (diffuse and half-cut) are also present in depth.

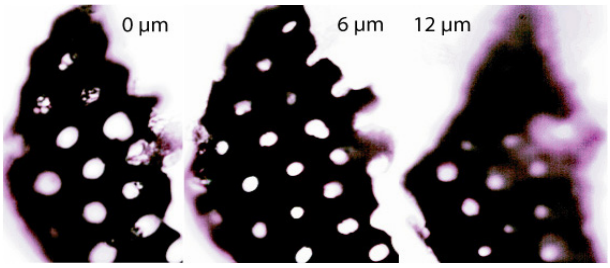

Figure 5: Carbon lamella focused on different depths (0µm - surface; 6µm and 12µm deep). The white points are diamonds.

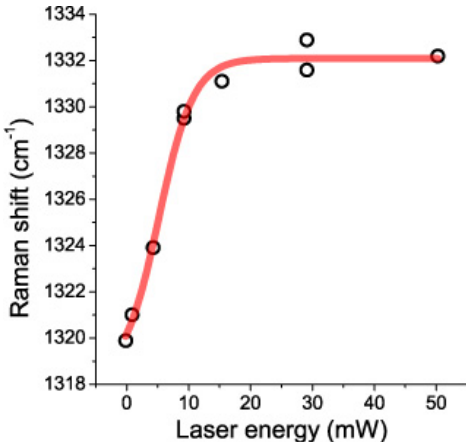

Figure 6: Sigmoid (Boltzmann) fit obtained for the diamonds in a DLC lamella, like Figure 5. The starting point is at 1318.3 and the end at 1332.1cm^{-1}, and the correlation coefficient R^2=0.99223.

The curve resembles roughly the Figure 1 for the reference diamond from Brazil. Only the FWHM values are relatively large (~70cm^{-1}) because different carbon components overlap (carbon, graphite, DLC, nano-diamonds, and diamonds). Even at a low laser energy of 4.3mW, the carbon is partially burned by heating (Figure 7).

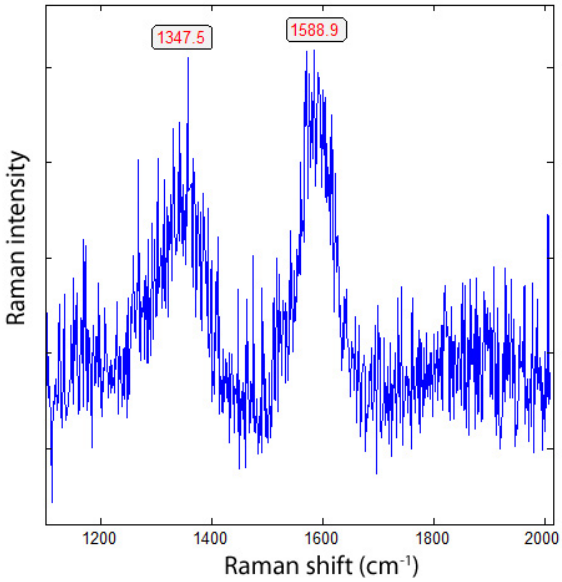

Figure 7: Raman spectrum of the lamella from Figure 5 between diamonds. The strong scattering results from the laser light destroying the carbon phases.

In rare cases, relatively sharp diamond and graphite lines were obtained (Figure 8).

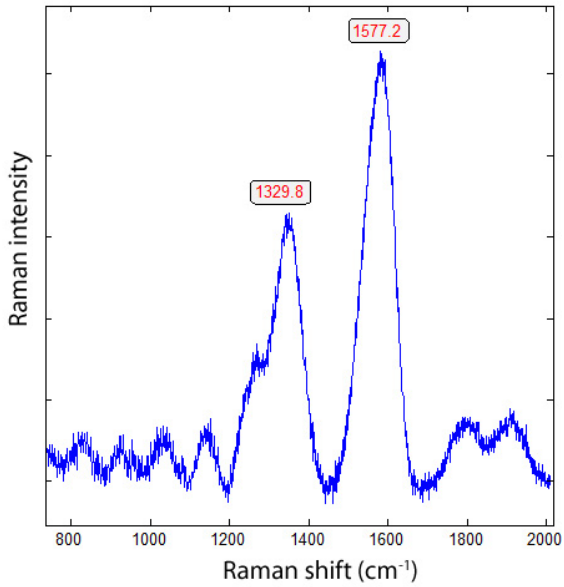

Figure 8: Raman spectrum of a diamond from the lamella in Figure 5.

Copyright © Rainer Thomas

The transparency of graphite-like carbon is astonishing. Because the depth-dependent appearance of the diamond inclusions results from optical sectioning in the strongly absorbing graphite matrix. Diamonds near the microscope's focal plane generate enhanced interfacial scattering or reflection and appear as white circular contrasts. Moving the focal plane through the approximately 30µm lamella reveals inclusions at progressively greater depths. That is not possible in graphite. However, according to Irmer and Dorner-Reisel [8], DLC films with a high sp^3/sp^2 ratio are transparent to visible light, as shown in Figures 4 & 5. That means the lamellae are not pure graphite but DLC. This phenomenon can explain the problems with the Raman spectra discussed in Brümmer et al. [3]. So, explain the so-called "impure" Raman spectra of the diamond spheres in the DLC lamellas. Figure 7 shows such a spectrum.

Conclusion

Our studies show that the diamonds in the DLC lamellas are real diamonds (Figure 6) with a large number of structural defects and a moderate sp^3/sp^2 ratio [8]. Besides diamond, DLC, and nanocrystalline diamond clusters, carbon/graphite lamellae are complexly built; however, they are rare formations during cooling of the grey cast iron sample. The exact time and temperature of formation of these diamond-bearing lamellas are unclear. Because the DLC lamellae are mostly completely impregnated with diamonds and nano-diamonds, we can assume that the diamond-bearing lamellae formed at equilibrium conditions of diamond/graphite. Because we do not know the exact formation temperature, we provisionally assume 1000 °C. If so, Day [9] gives a local pressure of about 4.5GPa. For grey cast iron, this is an exceptional value. Local high pressures are also indicated by colorless boron phases, as shown in Figure 9; [10]. At least the well-known iron phase diagrams do not show all stages of its cooling history.

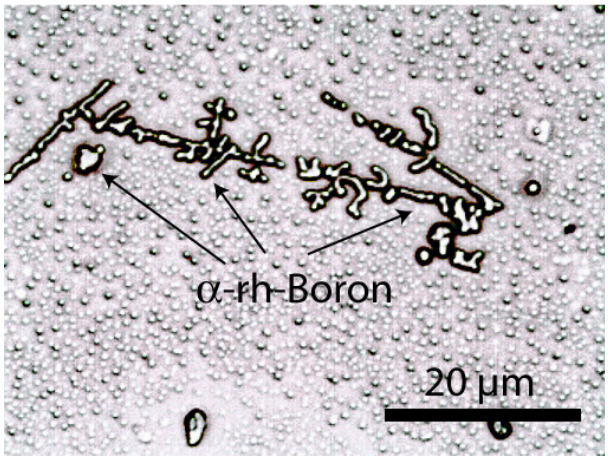

Figure 9: *α*-rhombohedral boron (*α*-rh-Boron) in the residue of iron sample 2. The small spheres in the background are micro-diamond and micro-boron spheres (2-4µm).

References

1. Thomas R (2025a) Formation of diamond in graphite of gray cast iron. GEMS 7(7): 1-4.
2. Thomas R (2025b) Gray cast iron or an iron meteorite: Preliminary results. GEMS 7(7): 1-3.
3. Brümmer G, Thomas R, Scheiblauer K (2026) The elixirs of metallurgy - on remarkably unnoticed phases in cast iron. Giesserei Rundschau 73(1): 6-22.
4. Thomas R, Davidson P, Rericha A, Recknagel U (2023) Ultrahigh-pressure mineral inclusions in acrustal granite. Evidence for a novel transcrustal transport mechanism. Geosciences 13: 1-13.
5. Parakhonskiy G (2012) Synthesis and investigation of boron phases at high pressure and temperature. Dissertation, University of Bayreuth, Germany, P. 111.
6. Solin SA, Ramdas AK (1970) Raman spectrum of diamond. Physical Review B 1(4): 1687-1698.
7. Triarhou LC (2009) Volume determination under the microscope, the simple way: the delesse-glagolev principle. Micscape Magazine, pp: 1-14.
8. Irmer G, Dorner-Reisel A (2005) Micro-Raman studies on DLC coatings. Advanced Engineering Materials 7(8): 694-705.
9. Day HW (2012) A revised diamond-graphite transition curve. American Mineralogist 97: 52-62.
10. Thomas R, Brümmer G, Scheiblauer K (2025) Unexpected carbon phases in grey cast iron - Diamond, calcite, and methane. GEMS 7(4): 1-6.

Copyright © Rainer Thomas